RESEARCH ARTICLE

In Vitro Behavior of a Novel Nanostructure Hardystonite/ Biphasic Calcium Phosphate Scaffolds (HT/BCPS); Evaluation and Investigation

Hassan Gheisari Dehsheikh

Department of Mechanical Engineering, Khominishahr Branch, Islamic Azad University, Khominishahr/ Isfahan, Iran

ARTICLE INFO

Article History:
Received 2021-01-09
Accepted 2021-04-03
Published 2021-05-01

Keywords:
Nanostructure
Hardystonite
Calcium phosphate
in vitro
TEM&SEM

ABSTRACT

In this study, highly porous almost (75%) nanostructured Hardystonite/biphasic calcium phosphate scaffolds (BCPS) with interconnected porosity was developed using various hardystonite (HT) contents via space holder technique. Transmission electron microscopy (TEM), X ray diffraction (XRD) and scanning electron microscopy (SEM) techniques was employed to evaluate different samples. In addition to, the agents of scaffold composition of mechanical behavior, bioactivity and biodegradability was studied. Also, the results showed that the produced scaffolds had an average pore size and density between 250-350 µm and 2.2 ± 0.4 - 1.7 ± 0.2 gr/cm3, respectively, depending on the Hardystonite (HT) with different contents. Furthermore, increasing the hardystonite content of scaffolds from 0 (control) to 30 wt. % enhanced the bioactivity test, biodegradability, and compressive strength from 1.1 ± 0.1 to 3.1 ± 0.2 MPa, respectively. Besides, MTT assay also confirmed that the BCPS30 (containing 30 wt. % of hardystonite) significantly promoted cell viability and cell adhesion compared to BCPS 0. Totally, our project suggests that nanostructured hardystonite/BCPS with improved biological and mechanical behavior (properties) could potentially be used for biomedical engineering such as bone tissue engineering application.

How to cite this article
Gheisari Dehsheikh H. In Vitro Behavior of a Novel Nanostructure Hardystonite/Biphasic Calcium Phosphate Scaffolds (HT/BCPS); Evaluation and Investigation. J. Nanoanalysis., 2021; 8(2): 86-100. DOI: 10.22034/jna.001.

INTRODUCTION

Scaffolds with desired biocompatibility, biodegradability and mechanical behavior have been a great interest to many scientists [1].The mechanical properties mismatch between bone and scaffolds can inversely affect the implant function in vivo. Bone tissue engineering is seeking to regenerate bone defects through combining cells, biocompatible scaffolds and growth factors. Scaffolds with poor mechanical properties may fail under load bearing applications; while scaffolds with higher mechanical behavior to that of bone may cause stress shielding, bone resorption and poor osseointegration [2]. Another crucial parameter that should be considered in the synthetic bone scaffolds is porosity. Pore size in the range of 150-600 µm is necessary for neovascularization, cell-migration [9, 3]. Natural hydroxyapatite with chemical formula $Ca10\ (PO_4)_6(OH)_2$, (NHA) is one of the best candidates to develop bone scaffolds for tissue engineering due to its unique properties such as good biocompatibility and chemical composition similar to that of bone [2,3,5]. Although, because of the low degradation rate as well as poor mechanical properties, various research has been conducted on the development of new bioceramics such as tri-calcium-phosphate (TCP),titania, and silicon-carbide with improved mechanical strength and biodegradability compared to pure hydroxyapatite (HA) [6,5,7]. Recently, Beta-tri-calcium-phosphate (ß-TCP) has great biocompatibility and biodegradability

* Corresponding Author Email: *Hassan.gh.d@gmail.com*

which resorbs faster than hydroxyapatite (HA) in the defect location and promote the healing process [9-10]. But of high bioactivity, osteoconductivity, and controllable degradation rate, BCP ceramics have been more favorable than pure HA and b-TCP alone, to repair periodontal defects or as bone graft replacements [10, 11, 12]. As regards, similar to other calcium phosphate ceramics (CPS) their strength are not acceptable for load bearing applications [6, 4, 12].

Recently, silicon-magnesium based bioceramics have drawn interest in the development of bone implant materials [15,16]. While zinc (Zn) is an essential element of bone, silicon (Si) is involved in human bone metabolism [16]. Hardystonite (HT) with the chemical formula of $Ca_2ZnSi_2O_7$ is a silicate-based bioceramic utilized for artificial bone and dental root as a result of its great hydroxyapatite formation ability and higher mechanical properties compared to HA [17,18,19]. The bending strength and fracture toughness of Hardystonite (HT) are 350 MPa and 3.5 MPa m1/2, respectively, which are 2-3 times higher than that of hydroxyapatite [19,20]. Furthermore, it has been reported that glassceramics consisting of eutectic phase, with the composition of 40 wt% TCP and 65 wt% hardystonite [21, 22].

Solid state sintering [23] and replication of polymer foams by impregnation [13,14]. On the other hand, biphasic calcium phosphate scaffolds (BCPS) have been successfully fabricated utilized camphene-based freeze-casting [8] and a combination of gel-casting and polymer sponge [6] techniques. Space holder approach has been widely used to develop metallic scaffolds. In this method, spacer particles such as carbamide (CO(NH2)2), ammonium hydrogen carbonate (NH4HCO3) and sodium chloride (NaCl) are mixed with the main powder to form porosity during the sintering process [24]. Also, limited ceramic based scaffolds have been fabricated using this method.

Finally, our aims of the present study was to produce nanostructured Hardystonite/biphasic calcium phosphate scaffolds (HT)/(BCPS) by space holder technique. Also, the influence of Hardystonite with different contents on the average pore size, porosity, microstructures and mechanical behavior of the scaffolds will be discussed. In addition to, the effects of (HT) nanopowder on the in situ formation of BCPS will be evaluated.

EXPERIMENTAL PROCEDURE

Formation of Hydroxyapatite (HA) and Hardystonite (HT) nanopowders

Hardystonite (HT) was via sol-gel technique based on the previous study [25]. In short, calcium nitrate tetrahedrate from Merk Co. and magnesium nitrate hexahydrate from Merk Co. with similar molarity (0.127M) was dissolved into 250 cc ethanol and sintered at 90 ˚C for 45 minutes. Tetraethyl orthosilicate (TEOS) (0.25 M) from Merk co were added to the above homogeneous solution and slowly stirred to obtain a gel network. The gel was dried at 110 ˚C for 36 hours and then calcium at 900 ˚C for 3 hours. The produced of powder were ball milled for 3 hours in a planetary ball-mill machine from Santam Sanat Co, in zirconia cup. Also,hydroxyapatite (HA) nonopowder were synthesized using the sol gel technique, according to previous study [6]. Appropriate amounts of Ca(NO3)2$4H2O and phosphoric pentoxide (from Merck Co) were separately dissolved in absolute ethanol to form 1.76 and 0.6 mol/l solutions, respectively. The two solutions were mixed and stirred at room temperature for 36 hours and then the obtained clear gel was dried at 90 C in an electrical oven for about 36 h. Dried gel were calcined at 800 C for 30 minutes in a muffle furnace by a heating rate of 6 C/min. Hydroxyapatite (HA) nanopowder was partially decomposed to tri-calcium phosphate (TCP) during sintering at high temperature.

Synthesis of Nanostructure Hardystonite/biphasic calcium phosphate scaffolds (HT/BCPS)

Hardystonite/BCPS was produced using a space holder technique. In the first part, as synthesized hydroxyapatite and Hardystonite nanopowders was blended with various weight ratio (100:0 , 90:10 , 80:20 and 70:30) in a high energy ball-milling (HEBM) for 2 h in a zirconia jar.

Also, in order to develop composite scaffolds (CS), sodium chloride (NaCl from Sigma Co) with a particle size of about 250-350 μm was used as spacer agent. Sodium chloride and composite powders with a weight ratio of 70:30 was mixed together. The prepared powder was uniaxially pressed into pellets in a hardened steel mould at a pressure of 300 MPa for 2 minutes using 6 wt% polyvinyl alcohol solution as a binder. The green bulks was annealed at 1200 C for 3 h with the

Table 1. Determination and characteristics of various scaffolds

Designation	Hardystonit Contents (wt%)	-TCP (wt%)ß	Apparent Porosity (AP%)	Real Density (RD %)(g/cm^3)	Apparent (Density AD)(%)
BCPS 0 (Control)	0	31	81 (±3)	3.14	1.7 (±0.4)
BCPS 10	10	24	81 (±1.4)	3.16	2.187 (±0.9)
BCPS 20	20	18	78 (±1.6)	3.18	2.5 (±0.14)
BCPS 30	30	14	75 (±4)	3.18	2.41 (±0.29)

heating and cooling rate of 3C/min in order to remove the NaCl particles. Totally, the samples was sintered at 1250 C for 3 h with heating and cooling rate of 5C/min. Table 1 showed the designation and specification of samples.

Investigation of nanopowders and scaffold
Survey of mechanical Characterization

In this part, for measure the strength of the samples with the height and diameter of 30 mm _ 20 mm were produced and then

subjected to a compression test using a universal testing machine (Sanam sanat Co, K40XV) at a crosshead speed of 0.6 mm/min. The

elastic modulus of each sample was calculated based on the Hooke's formula. For each category, three samples were examined and the mean value was reported. The results were expressed in terms of a mean value accompanied by a standard deviation.

Evaluation of In vitro bioactivity and biodegradability

In order to do this item, a simulated body fluid (SBF) containing ion concentration similar to those of human blood plasma was prepared according to a procedure described previously . The scaffold samples were soaking in simulated body fluid at 37˚C for 1,3,7,14,21 and 28 days. During the soaking time, the changes in the pH value of the solutions were calculated via a pH meter

(Hitachi, Japan). In addition to, the concentration of Calcium and Phosphorus ions in simulated body fluid was evaluated after soaking the scaffolds for 28 days using inductive coupled plasma (ICP, Zaies, Switzerland). After soaking, the scaffolds were dried at 60 ˚C for 1day. SEM and EDS were used to study the hydroxyapatite formation ability and morphology of precipitates on the surface of the scaffold samples. Degradation rate of scaffolds were investigated in buffered saline solution at pH ¼ 7.4 ± 0.03 and temperature of 36 ± 0.8 ˚C for 28 days. Buffer solution was changed every 3 days. In specific time intervals (7, 14, 21, and 28 days), the scaffolds were removed from the buffer solution, and dried in an electrical oven at 80 ˚C for 24 hours. Totally, the weight loss (wl %.) of the samples was calculated

as follows :

Survey of cell culture

The in vitro cytotoxicity of scaffold samples (BCPS0 and BCPS30) were evaluated based on the cell morphology and cell viability (3-(4,5-dimethylthiazol-2-yl)-2,5-diphenyltetrazolium (MTT)) assays. SAOS-2 cell line was purchased from the Pasteur Institute and cultured in Dulbecco's Modified Eagle Medium (KSWE, Germany) supplemented with 20% Fetal Bovine Serum (FBS, sdfaw, Germany) and 2% penicillin-streptomycin (sdfaw, Germany) under 6% CO2 at 37 ˚C. Also, before cell seeding, the cylindrical scaffolds (length 6 mm, diameter 5 mm) were sterilized for 10 h in 80% ethanol, and then rinsed three times with PBS (pH= 7.42 ± 0.04) and subsequently exposed to UV-light for 5 h. So, the scaffold samples were immersed in 300 mL of culture medium in a 98 well plate, overnight. After discarding the culture medium, the cells at a density of 6 × 10^3 cells per well were seeded on the samples as well as tissue culture plate and maintained at 37 ˚C under 6% CO2 condition for 7 days while the culture medium was refreshed every 3 days.

Another part was a survey of MTT test. MTTcolorimetric assay was performed to assess the cytotoxicity of the samples. Also, After 3 and 7 days of incubation, the culture medium was discarded and the wells were washed in PBS. The cell-seeded scaffold samples and control (tissue culture plate) (n = 3 per group) were incubated with the MTT solution (0.5 wt% MTT reagent in PBS) at 37 ˚C for 5 h. After aspiration of the MTT solution, the resultant blue formazan crystals were solubilized using 200 mL of dimethyl sulfoxide (WQAS, Sigma). In order to completely dissolve the crystals, the well plates were shaken smoothly for 30 min. Subsequently, 200 mL of dissolved formazan

solution of each sample was moved to 96-well plate and the optical density of each well, related to the number of living cells, was recorded using

a microplate reader (Biotech, Germany) against blank (KJHR) at a wavelength of 550 nm with a 645 nm reference filter. In addition to, the scaffold samples without cells were incubated under the same conditions and the optical density values were subtracated from values obtained via the corresponding scaffold-cell constructs. Totally, the mean and standard deviation for the triplicate wells of each sample were reported. The cell morphology was also investigated using scanning electron microscopy imaging. The cell seeded scaffolds were washed with PBS solution and fixed using 2% Glutaraldehyde (Merk Co.) solution at 37 ˚C for 4 h. So, the cell-seeded scaffolds were dehydrated through a graded series of ethanol (50% for 2 h and 750%, 80% and 100% each for 30 min) and dried at room temperature. Finally, the scaffolds were sputtered with a thin layer of gold and evaluated using microscope.

RESULTS AND DISCUSSION

Investigation of hydroxyapatite (HA) and Hardystonite (HT) nanopowders

Shows in Fig. 1 the X-ray diffraction patterns, scanning electron microscopy images and transmission electron microscopy of hydroxyapatite (HA) and Hardystonite (HT) nanopowders synthesized using sol gel method. Based on the XRD patterns, pure hydroxyapatite (XRD JCPDS data file No, 00-019-0239) (Fig. 1a) and Hardystonite (HT) (XRD JCPDS data file No. 01-003-0865) (Fig. 1b) nanopowders were synthesized without any secondary phases. In addition to, the average crystallite size of the (HA) and (HT) nano powders obtained via modified Scherer equation were about 19.8 ± 1 nm and 31.0 ± 2 nm, respectively. Also, the crystallinity of HA powder calculated from the XRD pattern using Eq. (5) were about 75%. As can be seen in Fig. 1c and

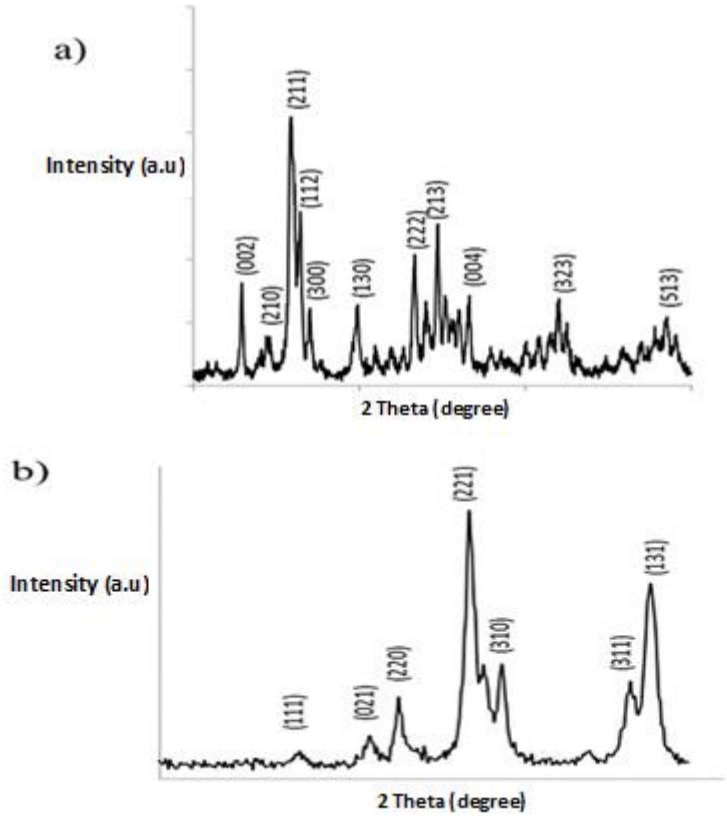

Fig. 1 X-Ray diffraction patterns (a , b), SEM images (c , d) and TEM micrographs (e , f) of HA (a, c, and e) and HT (b, d and f) nano-powders synthesized by sol gel method.

c)

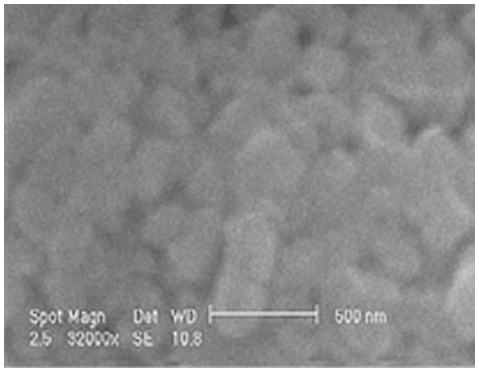

d)

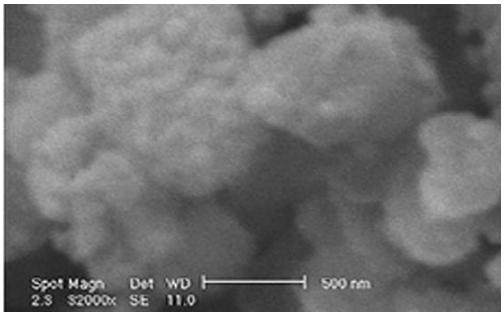

e)

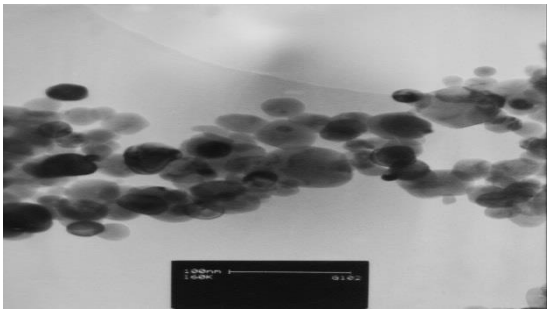

f)

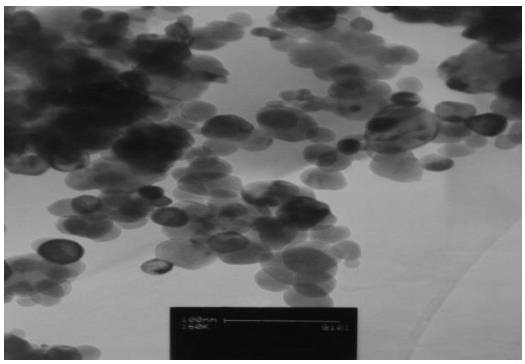

Continued Fig. 1 X-Ray diffraction patterns (a , b), SEM images (c , d) and TEM micrographs (e , f) of HA (a, c, and e) and HT (b, d and f) nanopowders synthesized by sol gel method.

d, HA and HT nanopowders showed a spherical morphology with the agglomerated particles smaller than 100 and 200 nm. As can be seen in the transmission electron microscopy (Fig. 1e and f), while the HA powder consisted of homogenous spherical particles with the average size of 18 ± 3 nm, the particles of HT powder were irregular in shape with the average size of 36 ± 2 nm.

Survey of composite scaffolds (CS)

The x-ray diffraction patterns of various scaffolds with different HT contents after sintering at 1250 ˚C for 3 h. According to the XRD patterns, all the composite consists of HA and beta-tri calcium phosphate (ß-TCP) as the main phases and a small amount of HT phase enhanced with increasing the content of HT nanopowder. So, the presence of ß-TCP in the XRD patterns demonstrated the decomposition of HA during the sintering at high temperature [7]. Furthermore, some ∝ -TCP peaks could be detected in all of the XRD pattern suggesting further phase transformation of ß-TCP phase is a low temperature polymorph of TCP which could be transformed to ∝ -TCP at high temperatures [22,21]. In addition to, the ratio of hydroxyapatite to ß -TCP varied in different compositions demonstrating the effects of HT contents on the decomposition degree of hydroxyapatite ceramic. Also, Table 1 shows the amounts of ß -TCP for various composites. As can be seen, with increasing the HT content the amount of ß -TCP decreased which is in a good agreement with the results obtained by other

researchers [23] who pointed out that incorporation of HT within HA matrix could suppress the decomposition of HA to TCP. Furthermore, HA/TCP ratio could be easily controlled via the addition of secondary agents such as HT in this research. So, based on the XRD patterns obtained from the scaffold samples (Fig. 2), the average crystallite size of HA in the composite scaffolds were about 31.0 ± 3.5, 32.0 ± 1.1, 28.0 ± 2.8 and 24.0 ± 3.1 nm for BCP based scaffolds consisting of 0, 10, 20 and 30 wt% of hardystonite (HT) nanopowder, respectively (Eq. (1)). The scanning electron microscopy images and pore size distribution of various scaffold samples were shown at Fig. 3 . Images with low magnification confirmed the formation of interconnected pores, which homogenously distributed throughout the samples. The average pores size of the scaffolds (Fig. 4a) reduced with increasing the HT content from 350 ± 80 µm to 200 ± 50 µm, which may boost bone ingrowth [24]. Higher magnification images also demonstrated the formation of micropores throughout the scaffolds. The histogram of micropore size was estimated by ImageJ software from the strut of the scaffolds (Fig. 3). As can be seen, the size of micropores reduced with increasing the Hardystonite (HT) content which can be ascribed to the improved sinterability of the scaffolds. The sintering temperature of the specimens was selected near the melting point of HT at 1300 ˚C [25]. Thus, HT nanopowder can act as

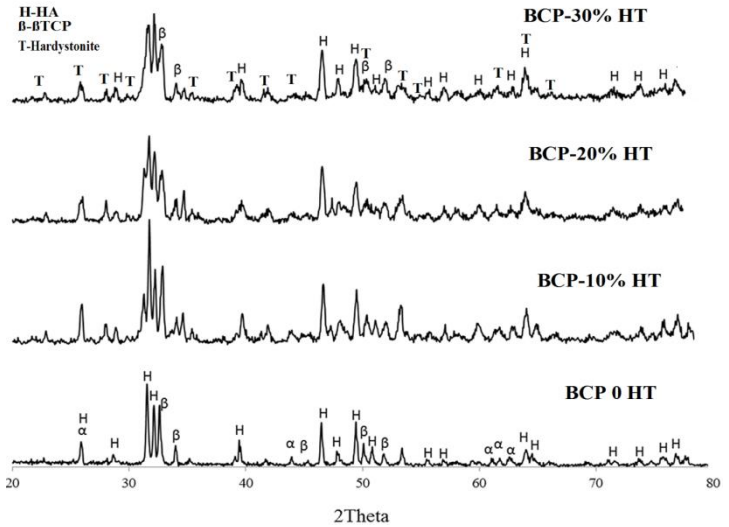

Fig. 2. X-Ray Diffraction patterns of the scaffolds consisting of various Hardystonite(HT) contents sintered at 1300 ˚C for 3 h.

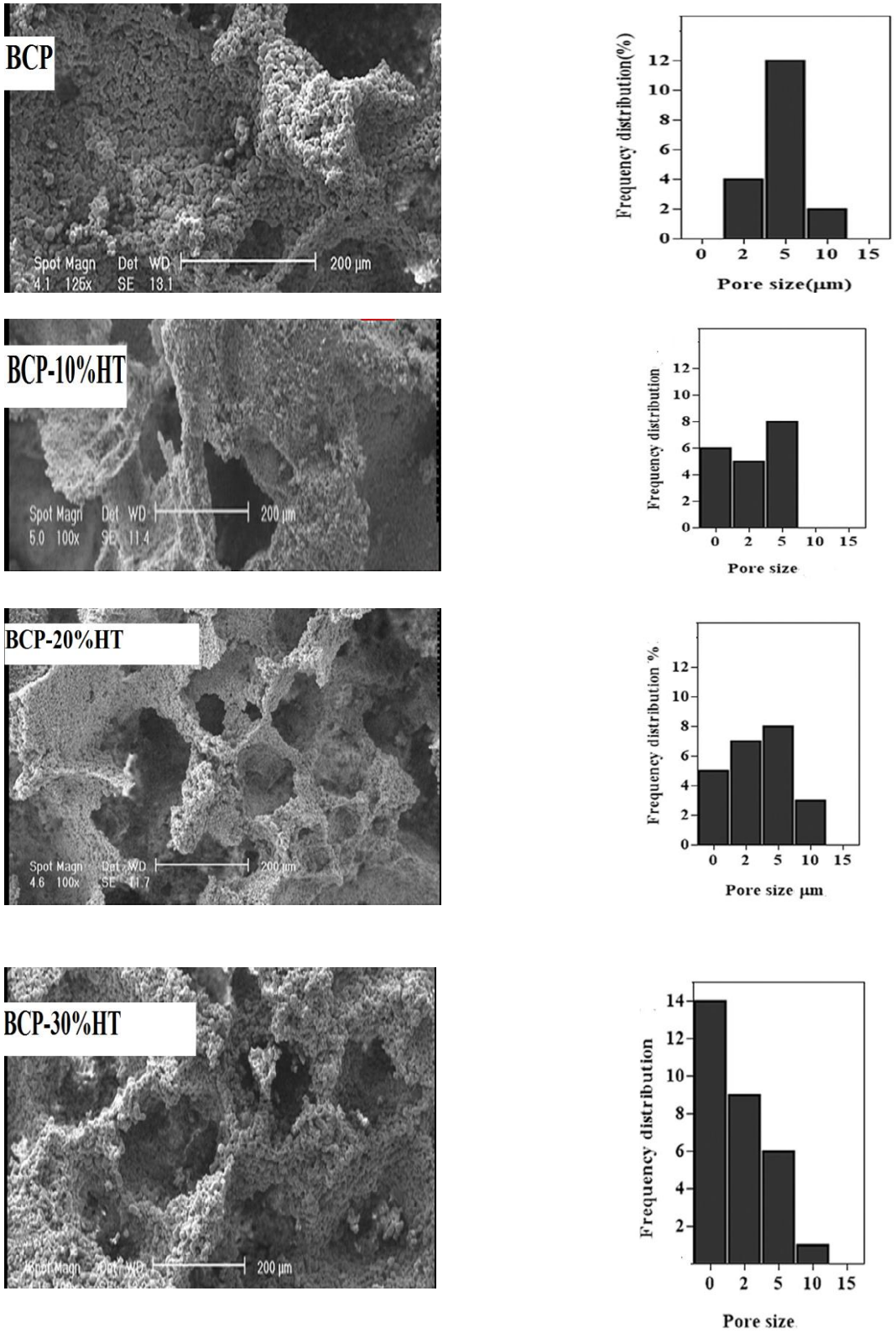

Fig. 3. Scanning electron microscopy images and micropores size of scaffolds sintered at 1300 ˚C for 3 h.

a sintering aid to improve the mechanical behavior of the scaffold samples. So, these result were in an excellent agreement with other studies, which reported the role HT in HT/HA bulk composites as a sintering agent [26]. Also, the average grain size of the scaffolds in different composites

also demonstrated the effects of HT on the suppression of grain growth (Fig4b). With increasing the HT content from 0 to 30 wt%, the average grain size of the scaffolds decreased from 7 ± 0.8 μm to 2 ± 0.5 μm, respectively. In order to, while biphasic calcium phosphate

grains started to necking, composite scaffolds were mostly densified, specifically at BCPS30 sample. The presence of HT in the BCPS matrix can simultaneously improve the sintering behavior and suppress the grain growth. Similar observations were reported in other studies regarding the presence of HT in alumina matrix which resulted in a decrease in the grain growth of alumina and an improvement in the densification rate [27]. You can see the average density and porosity of the scaffolds were calculated based on the Archimedes formula in (Table 1). The density of the scaffolds improved with increasing the HT content, confirming the role of HT agent in the reduction of micropores in the wall of scaffolds and improvement of scaffolds densification (Fig 3).Also, Fig. 5 shows the energy dispersive spectrometry mapping of Ca, P, Zn and Si elements in the BCPS30 scaffold after sintering at 1300 ˚C for 3 h. As you , HT nanopowder was well distributed in the BCP matrix. So, EDS micro-analysis demonstrated that NaCl particles were not remained in the scaffolds, hence this technique can be a suitable one for fabrication of ceramic based scaffolds. The Ca/P ratio obtained from the EDS analysis was about 1.42 which shows the decomposition of hydroxyapatite and the well distribution of HT phase in the constructs. The mechanical behavior of the scaffolds as a function of HT contents are shown in Fig. 6, The compressive strength of BCPS were in the ranges reported in the previous studies [6] and improved from 1.3 ± 0.3 MPa (BCPS control (0)) to 3.1 ± 0.4 MPa (BCPS30) via the addition of HT content up to 30 wt%. The mechanical behavior of synthetic scaffolds could be

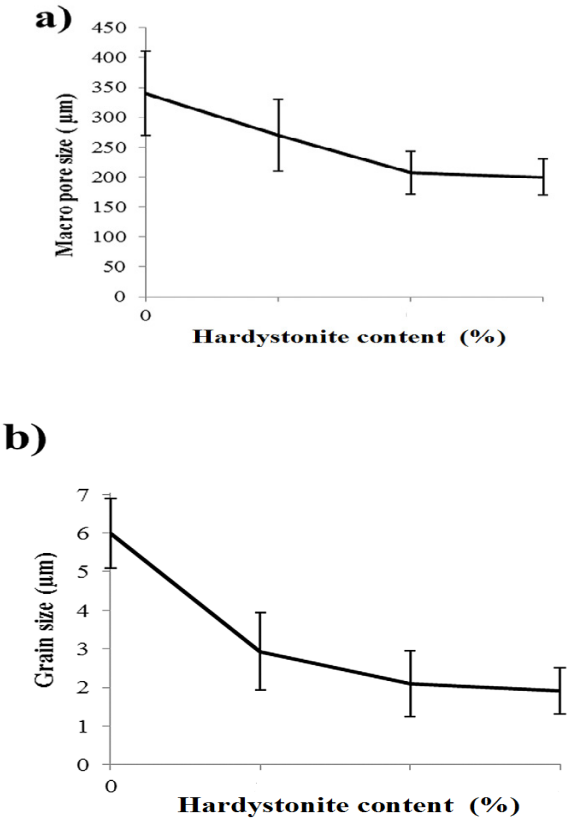

Fig. 4. Graphs of average a) macrospore and b) grain size of various composite scaffolds as a function of Hardystonite (HT) contents.

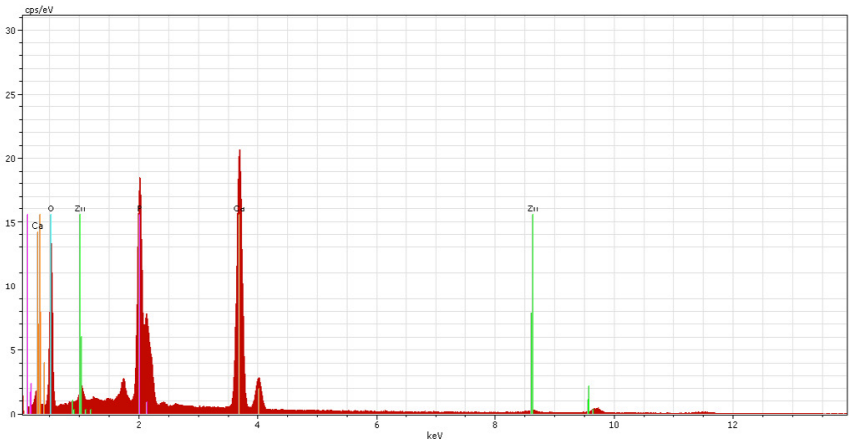

Element	series	[wt.%]	orm. wt.%]	orm. at.%]
Oxygen	K-series	43.08311	46.10041	67.0643
Silicon	K-series	0.770121	0.824056	0.682912
Phosphorus	K-series	10.61332	11.35661	8.533856
Calcium	K-series	36.87211	39.45442	22.91289
Zinc	K-series	2.116294	2.264507	0.806033
	Sum:	93.45495	100	100

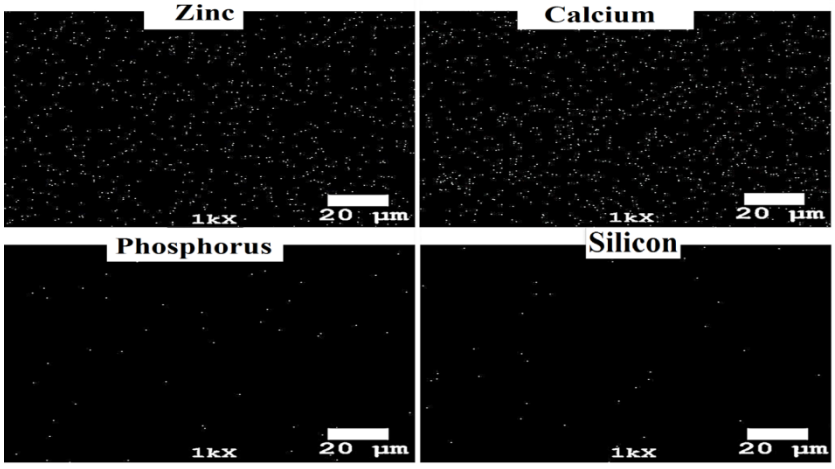

Fig. 5. Energy dispersive spectrometry mapping nanostructured BCPS 30 after sintering at 1300 °C for 3 h.

affected by their porosity, density, composition and grain size. So, on Table 1 and Fig. 4, introducing HT nanopowder into the BCPS matrix could act as a sintering aid leading to a smaller micropore size, and denser struts while preventing from grain growth during the sintering process. In order to, based on the results of this paper, decomposition of HA to TCP could be prohibited by adding HT to the matrix, which increased the mechanical behavior of the scaffold samples [16,28]. The success rate in bone replacement surgeries depends on the development of scaffolds with a compatible mechanical

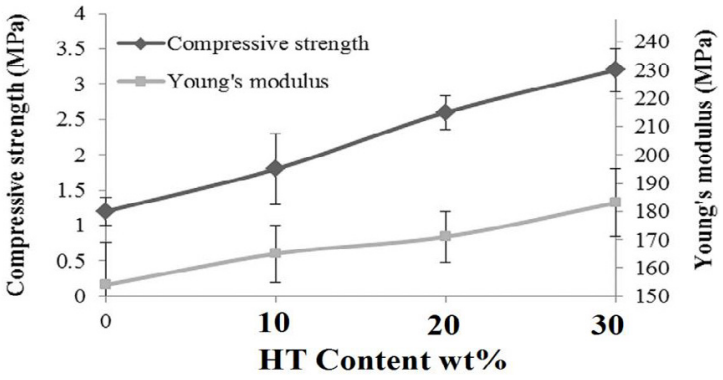

Fig. 6. Compressive modulus and strength of scaffolds as a function of HT contents

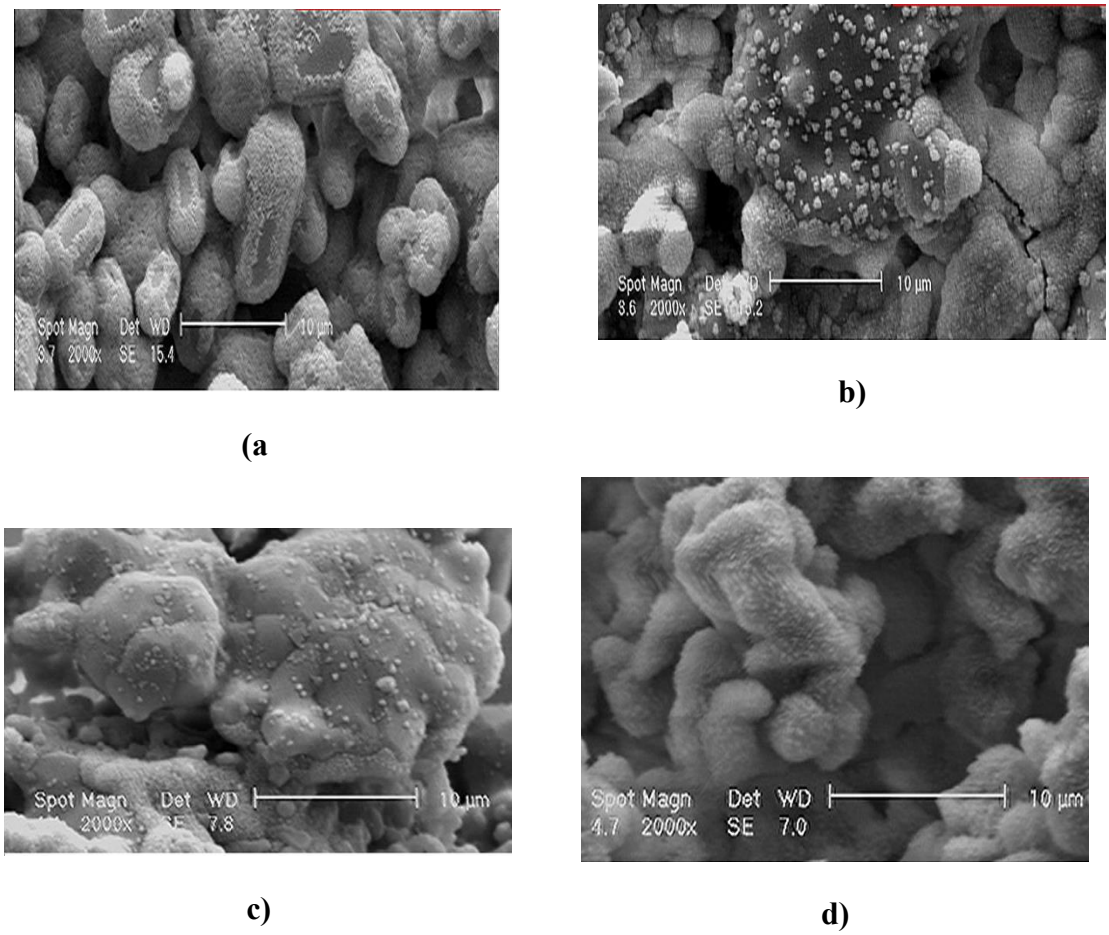

Fig. 7. Scanning electron microscopy images of a) BCP, b) BCPS-10, c) BCPS-20 and d) BCPS-30 after 28 days immersion in simulated body fluid with different resolutions

properties to that of bone acting as subtracts for cell growth. Due to the poor mechanical strength, HA scaffolds could be only used as a bone substitute in low loaded bearing applications [29]. In order to improve the mechanical behavior of HA based scaffolds, various kinds of composite scaffolds

have been developed. Furthermore, Hassan et al. [7] fabricated nanocomposite porous BCPS-10 wt% HA whisker scaffold with a porosity in the range of 72% using a combination of gel casting and polymer sponge technique. The mechanical properties of the scaffolds increased from 4 MPa (in BCPS) to 9.78 MPa (in BCPS-10% HA whisker scaffold). In this project, we revealed that the addition of HT nanopowder up to 30 wt% could significantly improve the compressive strength of BCPS. In order to, it is noteworthy to mention that a uniform microstructure is an important parameter for the higher mechanical properties of the scaffolds. The in vitro bioactivity of the scaffolds was evaluated using simulated body fluid (SBF) solution. The scanning electron microscopy images of the scaffolds with different compositions after soaking in the SBF solution for 28 days are presented in Fig. 7, Bone like apatite with spherical particles were deposited on the surface of the scaffolds. Therefore, increasing the HT content up to 30 wt% (Fig. 7d) boosted the HA formation on the surface of the scaffolds. The deposition of apatite layer on BCPS 30 after soaking in SBF for 28 days was confirmed via energy dispersive spectrometry spectrum (Fig. 8), Compared to the EDS spectrum of the scaffolds before immersing in SBF (Fig. 5), the concentration of P and Ca ions increased confirming the formation of HA layer on the surface of the scaffolds after soaking in SBF. Thus, Zn and Si ions were detected on the surface of the scaffold due to the presence of the HT phase. Fig. 9 a shows the changes of pH value of SBF during 28 days soaking of various scaffolds. The pH value of SBF were increased with increasing the HT content of the scaffolds. The pH changes graphs revealed two distinct regions; an increase in the pH up to 7 days of soaking time followed by a decrease in pH value. This behavior is in an agreement with the results obtained by other researchers who pointed out a similar trend in pH changes for other Silicate based ceramics such as wolastonite), HT [18] and bioglass [30]. Fig. 9 b shows Ca and P ion concentrations of simulated body fluid as a function of HT contents after 28 days of soaking. calcium ion concentration was increased from 17.4 ppm (BCPS0) to 29.32 ppm (BCPS10) and then decreased to 25.12 ppm (BCPS30). Calcium ions released from both BCPS and HT components, which resulted in an enhanced Ca ion concentration in SBF. Furthermore, the concentration of phosphorus ions reduced with increasing HT contents (Fig. 9 b) as a result of the formation of the supersaturated solution around the scaffolds and deposition of Ca and P ions on the surface which in turn implies the higher bioactivity of HT. It should be noted that rapid exchange of Ca^{2+} and Zn^{2+} ions with H^{+} or $H3O^{+}$ from simulated body fluid can increase the pH and hydroxyl concentration of the solution. These changes lead to the formation of Si-OH bonds on the surface of the scaffold which caused the nucleation of HA. In this part, migration of P, Ca and hydroxyl ions from the surrounding fluid to the surface of the scaffolds accelerated the nucleation of bone like HA and resulted in the reduction of pH value due to the feeding of hydroxyl ions during the formation of HA layer [21, 14]. The deposition of HA layer on the surface of the scaffolds could provide a suitable substrate for proliferation. Thus, a strong bond can be formed with the surrounding tissue and help the biological fixation of the scaffold in the bone defect [17]. In this research, the precipitation of HA layer on the surface of the composite scaffolds after soaking in SBF demonstrated a higher degree of bioactivity of composite scaffolds compared to that of BCPS. So, in the previous studies, a higher bioactivity was observed for CaO-SiO2-ZnO systems such as HT compared to calcium

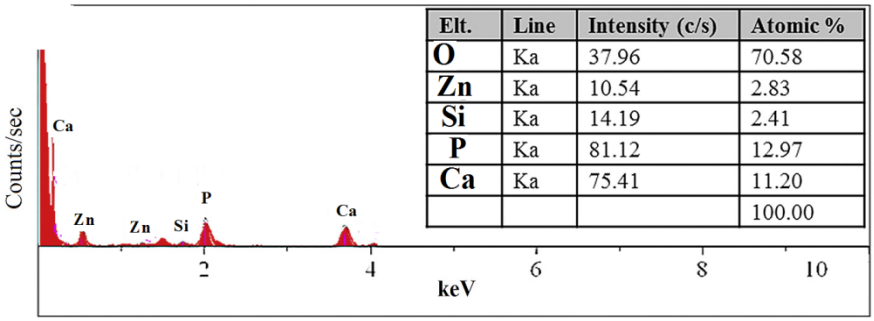

Elt.	Line	Intensity (c/s)	Atomic %
O	Ka	37.96	70.58
Zn	Ka	10.54	2.83
Si	Ka	14.19	2.41
P	Ka	81.12	12.97
Ca	Ka	75.41	11.20
			100.00

Fig. 8. Energy dispersive spectrometry spectrum of BCPS-30 after 28 days immersion in simulated body flouid.

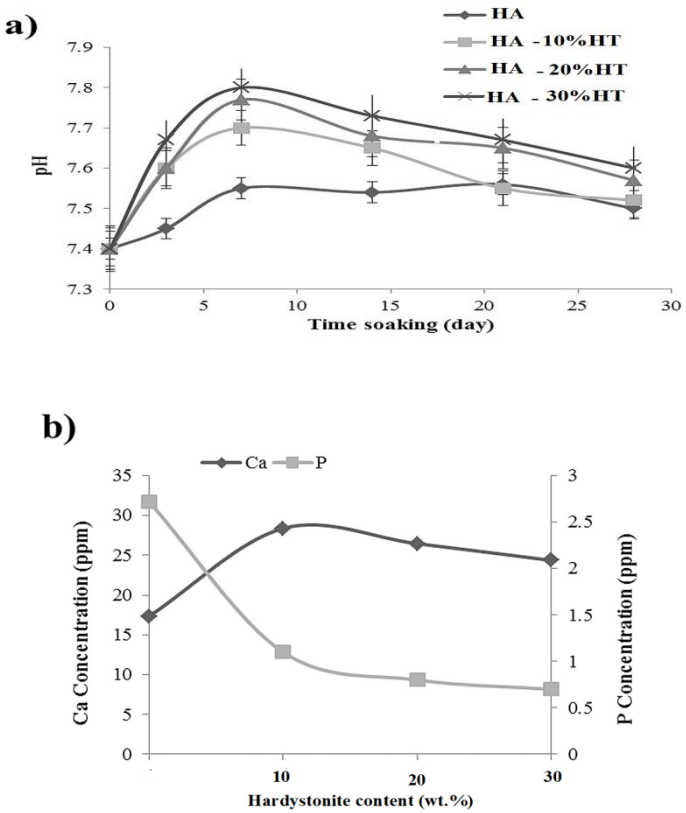

Fig. 9. a) pH value of SBF after immersion of various scaffolds as a function of soaking time. b) The concentration profiles of Calcium (Ca) and Phosphorus (P) ions in the SBF at different HT contents.

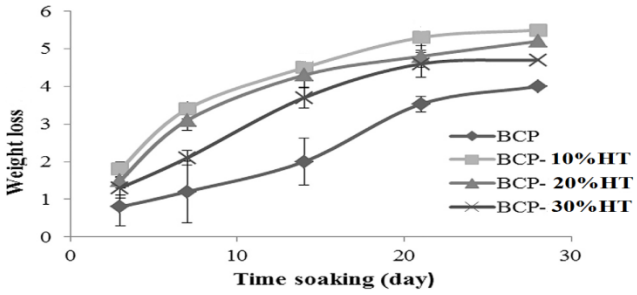

Fig. 10. The weight loss (wl.%) of different scaffolds in PBS solution as a function of soaking time.

phosphate (CP) ceramics [16,17].As you seen in Fig. 10 the weight loss of the scaffolds after soaking in PBS solution for up to 28 days. The weight loss (wl) of the scaffolds enhanced with increasing the soaking time and HT content which shows the higher degradation rate of the scaffolds. It is well proved that materials with smaller grain size show a higher degradation rate in vitro [31]. With increasing the HT content, the grain size of the scaffolds decreased in (Fig. 4 b) resulted in an increased interface between the samples and the solution which caused a higher degradation rate of

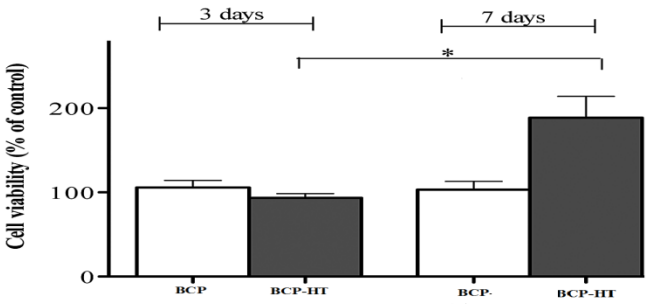

Fig. 11. Viability of SAOS-2 cells in contact with BCPS and BCPS - 30 after 3 and 7 days. (*: p < 0.05).

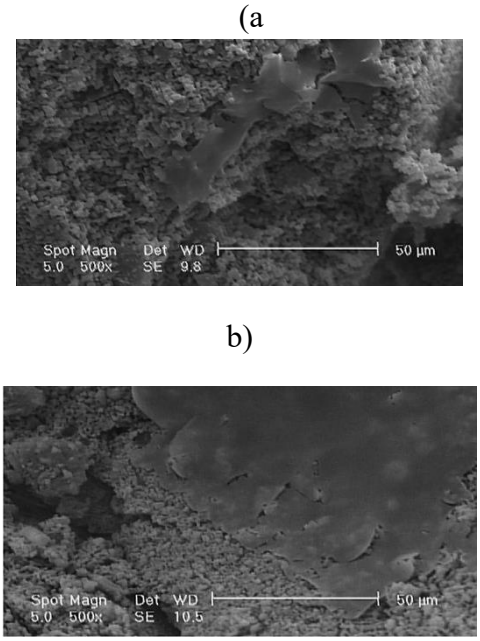

Fig. 12. The morphology of the cells cultured for 7 days on a) BCPS and b) BCPS 30 scaffolds.

the composite scaffolds. In addition to, the weight loss of the scaffolds produced in this research was lower than that of some bioceramics such as CaSiO3 (25%) [15] after soaking for 28 days, suggesting that these scaffolds can be used for bone defects which require a controlled slow degradation rate.

Furthermore, the viability of SAOS-2 cells in contact with BCPS0 and BCPS30 were evaluated after 3 and 7 days of culture using MTT

assay in (Fig.11). Due to the better physical and mechanical behavior of BCPS30 compare to other scaffolds, this scaffold were selected for the cytotoxicity evaluation. The results demonstrated that the number of live cells cultured on BCPS 30 significantly enhanced with increasing the culture time up to 7 days ($P < 0.04$). In addition to, cells on BCPS 30 showed a higher metabolic activity than cells on BCPS 0 scaffold ($P < 0.04$). Previous studies have also shown that Ca, Si, and Zn ions in ZnOSiO2CaO bioceramics could promote cell proliferation [17]. The higher metabolic activity could be due to the negative charge of silanol groups with lower isoelectric point, which formed appropriate cell-adhesive sites for proteins during culture and induced proliferation [32]. Also,Fig. 12 shows the SEM images of SAOS-2 cells on the BCPS0(control) and BCPS30 after 7 days. As you seen, cells were attached with a flat morphology on BCPS 30 , while BCPS0 did not support cell adhesion. Similarly,Hassan et al. [8] pointed out

that pure HT scaffolds support human osteoblastic like cell (HOB) adhesion with increasing the culture time. The addition of HT to BCPS plays a significant role in the cell adhesion and proliferations.

CONCLUSION

In present research work, Space holder method revealed a great potential to the development of porous ceramic scaffolds with a proper pore

size that is favorable for biomedical engineering such as bone tissue engineering applications. Furthermore, highly porous (75%) nostructured scaffolds were synthesized from hydroxyapatite (HA) and Hardystonite (HT) nanopowders by space holder. In addition to, adding HT nanopowder reduced the average pore and grain size of the scaffolds, which resulted in a three time enhancement in the compressive strength. Thus, the nanostructured composite scaffolds showed a higher bioactivity and biodegradability than pure BCPS. scaf Also, due to the positive role of silanol groups formed on the surface of the scaffolds, nanostructured HT/BCPS significantly promoted cell viability and proliferation compared to BCPS. So, the nanostructured composite scaffold of BCPS30 is cell friendly with suitable compressive strength, bioactivity and biodegradability which could be a promising scaffold for bone tissue engineering application.

CONFLICT OF INTEREST

All authors declare that no conflicts of interest exist for the publication of this manuscript.

REFERENCE

[1] C. Lieu, Z. Xia, J. Czernuszka, Design and development of three-dimensional scaffolds for tissue engineering, Chem. Eng. Res. Des. 85 (2007) 1051e1064.

[2] C. Shuai, J. Dieng, C. Gao, P. Feng, S. Peng, T. Xiao, Y. Deng, Mechanisms of tetra needle like ZnO whiskers reinforced Forsterite/bioglass scaffolds, J. Alloys Comp. 636 (2015) 341e347.

[3] H. Seitz, W. Rieder, S. Iersen, B. Leukers, C. Tille, Three-Dimensional printing of porous ceramic scaffolds for bone tissue engineering, J. Biomed. Mater. Res. Part B Appl. Biomater. 74 (2005) 782e788.

[4] A.J. Natheanael, J.H. Lee, D. Mangalaraj, S.I. Hong, Y.H. Rhee, Multifunctional properties of hydroxyapatite/titania bio-nano-composites: Bioactivity Antimicrobial Studies, Powder Technol. 228 (2012) 410e415.

[5] A.E. Hanneora, S. Ataya, Structure and compression strength of hydroxyapatite/ titania nanocomposites formed by high energy ball milling, J. Alloys Comp. 658 (2016) 222e233.

[6] R. Ramay, M. Zheang, Biphasic calcium phosphate nanocomposite porous scaffolds for load-bearing bone tissue engineering, Biomaterials 25 (2004) 5171e5180.

[7] Z. Niu, J. Zhang, S. Ren, Effect of whisker orientation on mechanical properties of hap-sicw composite bioceramics, J. Mater. Sci. Eng. 23 (2005) 1e3.

[8] A. Macechetta, I.G. Turner, C.R. Bowen, Fabrication of HA/TCP scaffolds with a graded and porous structure using a camphene-based freeze-casting metehod, Acta Biomater. 5 (2009) 1319e1327.

[9] S. Sancheez-Saelcedo, F. Balas, I. Izquierdo-Barba, M. Vallet-Reg, In vitro structural changes in porous HA/b-TCP scaffolds in simulated body fluid, Acta Biomater. 5 (2009) 2738e2751.

[10] X. Waneg, H. Fan, Y. Xiao, X. Zhang, Fabrication and characterization of porous hydroxyapatite/b-tricalcium phosphate ceramics by microwave sintering, Mater. Lett. 60 (2006) 455e458.

[11] S. Yamada, D. Heymann, J.M. Bouler, G. Daculsi, Osteoclastic resortption of calcium phosphate ceramic with different hydroxyapatite/b-tricalcium phosphate ratios, Biomaterials 18 (1997) 1037e1041.

[12] A.J. Amebard, L. Mueninghoff, Calcium phosphate cement: review of mechanical and biological properties, J. Prosthodont. 15 (2006) 321e328.

[13] S.I. Roohani-Esfaehani, S. Nouri-Khorasani, Z. Lu, R. Appleyard, H. Zreiqat, The influence hydroxyapatite nanoparticle shape and size on the properties of biphasic calcium phosphate scaffolds coated with hydroxyapatite/PCL composites, Biomaterials 31 (2010) 5498e5509.

[14] S.I. Roohani-Esfaehani, S. Nouri-Khorasani, Z. Lu, R. Appleyard, H. Zreiqat, Effects of bioactive glass nanoparticles on the mechanical and biological behavior of composite coated scaffolds, Acta Biomater. 7 (2011) 1307e1318.

[15] M. Kharazeiha, M.H. Fathi, Imeprovement of mechanical properties and biocompatibility of Forsterite bioceramic addressed to bone tissue engineering materials, J. Mech. Behav. Biomed. Mater. 3 (2010) 530e537.

[16] C. Sheuai, T. Liu, C.H. Gao, P. Feeng, T. Xiao, K. Yu, S.H. Peng, Mechanical and structural characterization of diopside scaffolds reinforced with grapheme, J. Alloys Comp. 655 (2016) 86e92.

[17] C. Wu, Y. Ramaswamy, H. Zreiquat, Porous diopside (CaMgSi2O6) scaffold: A promising bioactive material for bone tissue engineering, Acta Biomater. 6 (2010) 2237e2245.

[18] C. Wu, J. Chang, Deegradation, bioativity, and cytocompatibility of diopside, akermanite, and bredigite ceramics, J. Biomed. Mater. Res. Part B Appl. Biomater. 83 (2007) 153e160.

[19] T. Nonaemi, S. Tsutsumi, Study of dopside ceramics for biomaterials, J. Mater. Sci. Mater. Med. 10 (1999) 475e479.

[20] T. Noneami, Develoepmental-Study of diopside for use as implant material, Mater. Res. Soc. Symp. Proc. 252 (1992) 87e92.

[21] M. Ashiezuka, E. Ishida, Mechanical properties of silicate glass ceramics containing tricalcium phosphate, J. Mater. Sci. 32 (1997) 185e188.

[22] H. Ghmi, M.H. Faethi, H. Edris, Effect of the composition of hydroxyapatite/ bioactive glass nanocomposite foams on their bioactivity and mechanical properties, Mater. Res. Bull. 47 (2012) 3523e3532.

[23] Y.S. Kwoen, G. Son, J. Suh, K.T. Kim, Densification and grain growth of porous alumina compacts, J. Am. Ceram.

Soc. 77 (1994) 3137e3141.
[24] B. Arifvianto, J. Zhoeu, Fabrication of metallic biomedical scaffolds with the space holder method: a review, Materials 7 (2014) 3588e3622.
[25] L. Ghorbanian, R. Emeadi, M. Razavi, H. Shin, A. Teimouri, Synthesis and characterization of novel nano diopside bioceramic powder, JNS 2 (2012) 357e361.
[26] B.D. Cullity, Elemeents of X-ray Diffraction, second ed., Addison-Wesley, 1978.
[27] Y.X. Pang, X. Beao, Influence of temperature, Ripening Time and Calcination on the Morphology and Crystallinity of Hydroxyapatite Nanoparticles, J. Eur. Ceram. Soc. 23 (2003) 1697e1704.
[28] A. Moneshi, P.F. Meseser, Quantitative phase analysis in Industrial research, J. Mater. Sci. 26 (1991) 3623e3627.
[29] D.R. Askeeland, The Science and Engineering of Materials, second ed., PWS, 1989.
[30] M. Bohener, J. Lemaitre, Can bioactivity be tested in vitro with SBF solution Biomaterials 30 (2009) 2175e2179.
[31] M. Dieba, M. Kharaziha, M.H. Fathi, M. Gholipourmalekabadi, A. Samikuchaksaraei, Preparation and characterization of polycaprolactone/
forsterite nanocomposite porous scaffolds designed for bone tissue regeneration, Comp. Sci. Tech. 72 (2012) 716e723.
[32] A. Taempieri, G. Celotti, F. Szonetagh, E. Landi, Sintering and characterization of HA and TCP bioceramics with control of their strength and phase purity, J. Mater. Sci. Mater. Med. 8 (1997) 29e37.